Progress In Electromagnetics Research, PIER 92, 17–32, 2009

THICKNESS-INDEPENDENT AUTOMATED CONSTITUTIVE PARAMETERS EXTRACTION OF THIN SOLID AND LIQUID MATERIALS FROM WAVEGUIDE MEASUREMENTS

U. C. Hasar †

Department of Electrical and Electronics Engineering
Ataturk University
Erzurum 25240, Turkey

Abstract—The constitutive parameters measurement of thin solid and liquid materials by transmission-reflection methods generally suffers from a) the requirement of the transformation of measured scattering parameters from the reference plane to the end surfaces of the material (measurement plane) and b) inaccurate knowledge on the length of the material, if the material does not fill the entire measurement cell (a waveguide or coaxial-line section). In this research paper, a microwave waveguide method for constitutive parameters determination of these materials is proposed to simultaneously eliminate these problems. There are three main advantages of the proposed method as: a) it explicitly determines the constitutive parameters from measured S-parameters; b) it does not require the knowledge about sample length since it directly measures it as a by-product of the method; and c) it offers a self-checking feature to trace the performance and accurateness of measurements. This feature does not depend on the constitutive parameters of the sample. We measured the complex permittivity of some thin solid and liquid test samples for validation of the method.

1. INTRODUCTION

Microwave methods have extensively been used for materials' electrical characterization in industries such as civil, aerospace, electronics, chemical, and etc. [1–4]. These methods can be divided into two groups

Corresponding author: U. C. Hasar (ugurcem@atauni.edu.tr).
† Also with Department of Electrical and Computer Engineering, Binghamton University, Binghamton 13902, NY, USA.

as a) resonant and b) nonresonant methods [2]. Resonant methods have much better accuracy and sensitivity than nonresonant methods [5] and are generally applied to characterization of low-loss materials. In a recent study, it has been shown that these methods are also applicable to high-loss materials provided that very small samples are prepared or higher volume cavities are constructed [6]. However, a meticulous sample preparation is needed before measurements. In addition, for an analysis over a broad frequency band, a new measurement set-up (a cavity) must be made, which is not feasible in a practical point of view. Tunable resonators can be used for a wider frequency band analysis; nonetheless, they are expensive and an increase in the frequency bandwidth accompanies a decrease in the accuracy [7]. On the other hand, nonresonant methods have relatively higher accuracy over a broad frequency band and necessitate less sample preparation compared to resonant methods. Additionally, they allow the frequency-domain or time-domain analysis [8], or both.

The transmission-reflection nonresonant methods are the most commonly used methods due to their simplicity and broadband frequency coverage [9–14]. When applying these methods for measurements of liquid materials, some form of approximation in the physical nature of the measurement apparatus and/or forward and inverse problem formulations are generally made [14, 15] or formulations require that the dielectric specimen be low-loss [16]. To avoid any meniscus formation on top of liquid samples, generally the measurement set-up is positioned vertically [17, 18]. However, this will not help much, since planar measurement planes may not be easily achieved [14] and eventually this circumstance can degrade the measurement performance.

Coaxial sample holders can be utilized for broadband measurements [19]; however, they suffer from a bad contact between the sample and coaxial inner and outer conductors [20, 21]. On the other hand, if a coaxial line sample holder is used and dimensioned so that only single mode operation is possible, the dimensions become small and meniscus and other dimensional uncertainties may adversely affect the measurements [22]. Because waveguide measurements are highly sensitive, sample preparation for these measurements is relatively easy, and mechanical connections of waveguide sections are simple and robust, waveguide sample holders have effectively been applied for precise and accurate dielectric characterization of liquid samples [14, 15, 17, 18, 22, 23].

A self-checking method was proposed for waveguide measurements of samples' constitutive parameters (relative complex permittivity, ε_r, and relative complex permeability, μ_r) [22]. Although this method

auto-monitors the accuracy of measurements, it may not be applicable to liquid materials because of meniscus formation. To circumvent this problem, a waveguide holder for liquid materials sandwiched between two dielectric plugs has recently been proposed [14]. Even though this method includes the effect of plugs in theoretical formulations, it has two drawbacks. First, it requires precise knowledge on the location of the sample in-between the plugs inside the waveguide in order to eliminate the effect of large measurement errors arising from a shift in the calibration plane. Amplitude-only measurements can be used for this goal [24–27]. While the methods in [24, 26] and in [25], respectively, consider low-loss and high-loss materials with substantiate lengths, that in [27] proposes a method for electrical characterization of thin low-loss materials. Although these methods are attractive, they suffer from sagging of solid thin materials or are not applicable to electrical characterization (ε_r and μ_r) of low-loss liquid materials. In addition, these methods are not sufficient to fully characterize the electrical properties of materials since the relation between the constitutive parameters and the measured scattering (S-) parameters are not direct [28]. Second, it suffers from inaccurate knowledge on sample thickness. This is really a big problem for liquid samples since they occupy the space in which they are poured, resulting in a varying sample thickness for different containers.

The effects of inaccurate knowledge about the constitutive parameters and thickness of plugs, which are used for holding the liquids, on measurements can be removed by including the plugs in the calibration process [29]. However, this technique may decrease the measurement performance for the following reasons. First, for each different sample length or for various samples, this calibration should be repeated which is not feasible. This is especially a big problem for liquid samples whose specific gravity is not known. Second, the measured level of the transmission S-parameter may be lower than the threshold of the measuring instrument for lossy samples whose electrical properties are not yet known. In this circumstance, the calibration should be performed for thinner samples, which is time consuming.

In this research paper, we propose a different waveguide method and present different formulations which eliminate the measurement plane dependency of constitutive parameters of solid and liquid materials from measurements and include the effects of plugs used for holding the materials inside the holder. The advantages of the proposed method are that it does not require any knowledge on the length of the sample and it eliminates the effects of any shift in the measurement plane on measurements. In addition, it

allows flexible measurements since the measurement set-up could be horizontally or vertically positioned. Furthermore, the proposed method determines the constitutive parameters without using any zero-search algorithm [30]. Finally, it proposes a self-checking feature for monitoring the accuracy and performance of measurements before starting the constitutive parameters extraction.

2. THE METHOD

2.1. Problems in Constitutive Parameters Measurement of Thin Materials

The problem for ε_r and μ_r measurement of a thin material with length L inside a rectangular waveguide sample holder is depicted in Fig. 1. While the configuration in Fig. 1 does not change across x-axis, it changes over y-axis and z-axis. In the analysis, it is assumed that the sample is isotropic, symmetric and homogenous. The theoretical analysis is performed for each region (Regions I–III) in Fig. 1.

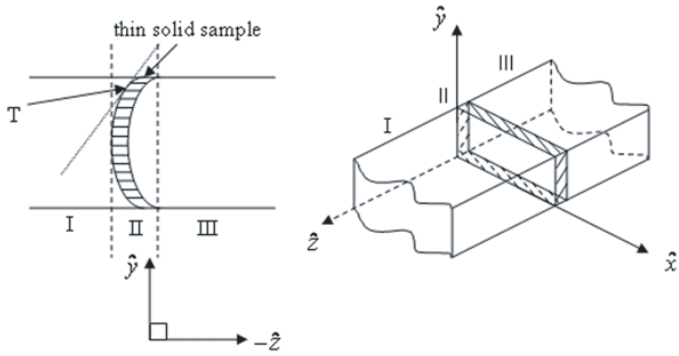

Figure 1. The problem for constitutive parameters measurement of thin solid samples.

It is assumed that the wave propagates through Region I in $-z$-direction with the dominant mode (TE_{10}). For the problem in Fig. 1, expressions of electric and magnetic fields for each region can be derived from their vector potentials (or Hertzian vectors), $\vec{A}$ and $\vec{F}$, such as [31]

$$\vec{E}^{(n)} = -j\left\{\omega\vec{A}^{(n)} - \frac{1}{\omega\mu_{(n)}\varepsilon_{(n)}}\nabla\left(\nabla\cdot\vec{A}^{(n)}\right)\right\} - \frac{1}{\varepsilon_{(n)}}\nabla\times\vec{F}^{(n)}, \quad (1)$$

$$\vec{H}^{(n)} = -j\left\{\omega\vec{F}^{(n)} + \frac{1}{\omega\mu_{(n)}\varepsilon_{(n)}}\nabla\left(\nabla\cdot\vec{F}^{(n)}\right)\right\} + \frac{1}{\mu_{(n)}}\nabla\times\vec{A}^{(n)}, \quad (2)$$

where n = I, II and III, ω is the angular frequency, and $\varepsilon_{(n)} = \varepsilon'_{(n)} - j\varepsilon''_{(n)}$ and $\mu_{(n)} = \mu'_{(n)} - j\mu''_{(n)}$ are the complex permittivity and complex permeability of each region. For the incident fields in Region I, we can assume that $\vec{A}^{(I)+} = 0$ and $\partial F_z^{(I)+}/\partial y = 0$ where the superscript '+' denotes the incident wave. Besides, in Region II, both electric vector potential and magnetic vector potential must exist in order to apply the continuity conditions at sample-air interface for each portion on sample surfaces (for example, the point T in Fig. 1). In addition, $\varepsilon_{(\mathrm{II})}$ and $\mu_{(\mathrm{II})}$ change from location to location in Region II. This circumstance results in TE and TM modes not only in Region II but also Regions I and III. As a result, we can write

$$F_{z(\mathrm{I})} = C_1 \cos\left(\frac{\pi x}{a}\right) e^{\gamma_{01} z} + C_{\mathrm{I}mn} \cos\left(\frac{m\pi x}{a}\right) \cos\left(\frac{n\pi y}{b}\right) e^{-\gamma_{02} z} \quad (3)$$

$$A_{z(\mathrm{I})} = D_{\mathrm{I}ku} \sin\left(\frac{k\pi x}{a}\right) \sin\left(\frac{u\pi y}{b}\right) e^{-\gamma_{02} z} \quad (4)$$

$$F_{z(\mathrm{II})} = \cos\left(\frac{m\pi x}{a}\right) \cos\left(\frac{n\pi y}{b}\right)\left(C^{+}_{\mathrm{II}mn} e^{\gamma(y,\,z) z} + C^{-}_{\mathrm{II}mn} e^{-\gamma(y,\,z) z}\right), \quad (5)$$

$$A_{z(\mathrm{II})} = \sin\left(\frac{k\pi x}{a}\right) \sin\left(\frac{u\pi y}{b}\right)\left(D^{+}_{\mathrm{II}ku} e^{\gamma(y,\,z) z} + D^{-}_{\mathrm{II}ku} e^{-\gamma(y,\,z) z}\right), \quad (6)$$

$$F_{z(\mathrm{III})} = \cos\left(\frac{m\pi x}{a}\right) \cos\left(\frac{n\pi y}{b}\right)\left(C^{+}_{\mathrm{III}mn} e^{\gamma_{02} z} + C^{-}_{\mathrm{III}mn} e^{-\gamma_{02} z}\right), \quad (7)$$

$$A_{z(\mathrm{III})} = \sin\left(\frac{k\pi x}{a}\right) \sin\left(\frac{u\pi y}{b}\right)\left(D^{+}_{\mathrm{III}ku} e^{\gamma_{02} z} + D^{-}_{\mathrm{III}ku} e^{-\gamma_{02} z}\right), \quad (8)$$

where m, n, k and u are mode numbers; C_1, $C_{\mathrm{I}mn}$, $D_{\mathrm{I}ku}$, $C^{+}_{\mathrm{II}mn}$, $C^{-}_{\mathrm{II}mn}$, $D^{+}_{\mathrm{II}ku}$, $D^{-}_{\mathrm{II}ku}$, $C^{+}_{\mathrm{III}mn}$, $C^{-}_{\mathrm{III}mn}$, $D^{+}_{\mathrm{III}ku}$ and $D^{-}_{\mathrm{II}ku}$ are constants and

$$\begin{aligned} m &= 0,\, 1,\, 2,\, \ldots \quad n = 0,\, 1,\, 2,\, \ldots \quad m = n \neq 0, \\ k &= 1,\, 2,\, 3,\, \ldots \quad u = 1,\, 2,\, 3,\, \ldots \end{aligned} \quad (9)$$

$$\begin{aligned} \gamma_{0y} &= j\frac{2\pi}{\lambda_0}\sqrt{1 - f_{cy}^2/f^2}, \quad y = 1,\, 2, \\ \gamma(y,\, z) &= j\frac{2\pi}{\lambda_0}\sqrt{\varepsilon_r\,(y,\, z)\,\mu_r\,(y,\, z) - f_{c3}^2/f^2}, \end{aligned} \quad (10)$$

$$\begin{aligned} f_{c1} &= \frac{c}{2a}, \quad f_{c2} = \frac{c}{2\pi}\sqrt{\left(\frac{m\pi}{a}\right)^2 + \left(\frac{n\pi}{b}\right)^2}, \\ f_{c3} &= \frac{c}{2\pi\sqrt{\varepsilon_r(y,z)\mu_r(y,z)}}\sqrt{\left(\frac{k\pi}{a}\right)^2 + \left(\frac{u\pi}{b}\right)^2}. \end{aligned} \quad (11)$$

Here, f, f_{c1}, f_{c2}, and c are, respectively, the operating and cut-off frequencies in Regions I (or III) and II and the speed of light; λ_0 corresponds to the free-space wavelength and $\varepsilon_r(y, z)$ and $\mu_r(y, z)$ are the relative complex permittivity and relative complex permeability of Region II, which both depend on y-axis and z-axis. Using the electric vector potentials in (3)–(8), electric and magnetic fields can be determined from (1) and (2) for each Region (I, II and III). If the problem given in Fig. 1 took into account the change in all axes in Region II, ε_r, μ_r and γ would all change with all axes.

2.2. Derivation of Complex *S*-Parameters

Since the measurement of ε_r and μ_r requires consideration of different TE and TM modes, this process greatly increases the computation time [32]. In this research paper, to decrease this time we propose a waveguide geometry for ε_r and μ_r measurement of a sample sandwiched between stable and movable plugs, as shown in Fig. 2.

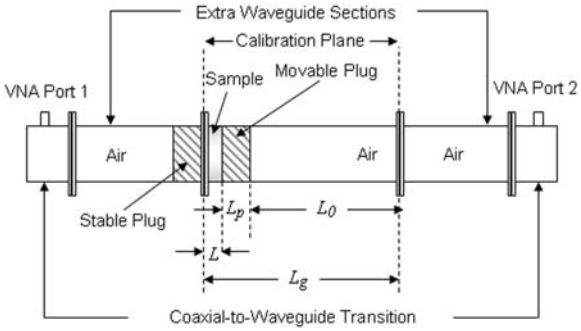

Figure 2. The geometry for constitutive parameters measurement of thin solid and liquid samples by the proposed method (VNA denotes the vector network analyzer).

We assume that the plugs are homogenous, isotropic and flat. With this configuration, we can neglect the TE and TM modes arising from the unevenness of the sample surface. In the theoretical calculation in this subsection, we also assume that a single-mode transmission (TE_{10}) occurs between reference planes in Fig. 2. It is well known that if the real part of the relative complex permittivity of the sample or movable plug can be greater than 4, higher-order modes will appear as a result of different cut-off frequencies in (11) [33]. Using samples and dielectric plugs with a thickness less than one-half guided wavelength of the fundamental mode will suppress these modes [13].

Another option could be using two extra waveguide sections with lengths greater than 70 mm (greater than two free-space wavelengths) between the reference planes and coaxial-to-waveguide adapters for thick samples [12, 21–24]. This is because higher-order modes will die out drastically in a short distance away from the sample and real measurements are performed near the adapters [22].

Using the electric vector potential in (3) for expressing electromagnetic fields and applying boundary conditions (continuity of electric and magnetic fields) on plug and sample surfaces, the forward and reverse S-parameters at reference planes are expressed as

$$S_{11} = \frac{(\Gamma_s - \Gamma_p)\left(1 - \Gamma_p\Gamma_s T_p^2\right) + \left(\Gamma_p T_p^2 - \Gamma_s\right)(1 - \Gamma_p\Gamma_s)\, T_s^2}{\left(1 - \Gamma_p\Gamma_s T_p^2\right)(1 - \Gamma_p\Gamma_s) + (\Gamma_s - \Gamma_p)\left(\Gamma_p T_p^2 - \Gamma_s\right) T_s^2}, \quad (12)$$

$$S_{22} = \frac{(1 - \Gamma_p\Gamma_s)\left(\Gamma_s T_p^2 - \Gamma_p\right) T_0^2 + \left(\Gamma_s - T_p^2\right)(\Gamma_s - \Gamma_p)\, T_s^2 T_0^2}{\left(1 - \Gamma_p\Gamma_s T_p^2\right)(1 - \Gamma_p\Gamma_s) + (\Gamma_s - \Gamma_p)\left(\Gamma_p T_p^2 - \Gamma_s\right) T_s^2}, \quad (13)$$

$$S_{21} = \frac{\left(1 - \Gamma_s^2\right)\left(1 - \Gamma_p^2\right) T_s T_p T_0}{\left(1 - \Gamma_p\Gamma_s T_p^2\right)(1 - \Gamma_p\Gamma_s) + (\Gamma_s - \Gamma_p)\left(\Gamma_p T_p^2 - \Gamma_s\right) T_s^2}, \quad (14)$$

where

$$\Gamma_p = \frac{\gamma_p - \gamma_{01}\mu_p}{\gamma_p + \gamma_{01}\mu_p}, \quad \Gamma_s = \frac{\mu_r\gamma_p - \mu_p\gamma}{\mu_r\gamma_p + \mu_p\gamma}, \quad (15)$$

$$T_p = \exp\left(-\gamma_p L_p\right), \quad T_s = \exp\left(-\gamma L\right), \quad T_0 = \exp\left(-\gamma_{01} L_0\right), \quad (16)$$

$$\gamma_p = j\frac{2\pi}{\lambda_0}\sqrt{\varepsilon_p\mu_p - \left(\frac{f_{c1}}{f}\right)^2}, \quad \gamma = j\frac{2\pi}{\lambda_0}\sqrt{\varepsilon_r\mu_r - \left(\frac{f_{c1}}{f}\right)^2}. \quad (17)$$

Here, Γ_p, T_p, Γ_s, and T_s are, respectively, the first reflection and transmission coefficients of the movable plug- and the sample-filled cells; T_0 is the propagation factor in the air-filled cell; γ_p, and γ represent the propagation constants of the movable plug- and the sample-filled cells; ε_p, μ_p, ε_r, and μ_r are, respectively, the relative complex permittivities and permeabilities of the movable plug and the sample; and L_p and L_0 denote the lengths of the movable plug and the air section inside the waveguide in Fig. 2.

2.3. Elimination of the Dependency of Calibration-plane

It has been known for many years that the measurements of S_{11}, S_{21}, and S_{22} create a over-determined system of nonlinear equations for evaluation of ε_r and μ_r. The motivation of our study is to derive explicit expressions for ε_r and μ_r determination using the

measurements of S_{11}, S_{22}, and S_{21} (or S_{12}) when L_0 and L are unknown.

It is clearly seen from (12)–(14) that while S_{21} and S_{22} are dependent on calibration plane, S_{11} is not a function of T_0. Thus, using (13) and (14), we eliminate T_0 in a simple manner as

$$S_\Delta = S_{21}^2/S_{22} = \left[\left(1-\Gamma_s^2\right)^2 (1-\Gamma_p)^2 T_s^2 T_p^2\right]/\Lambda_1\Lambda_2. \tag{18}$$

where

$$\Lambda_1 = (1-\Gamma_p\Gamma_s)\left(\Gamma_s T_p^2 - \Gamma_p\right) + \left(\Gamma_s - T_p^2\right)(\Gamma_s - \Gamma_p)\, T_s^2, \tag{19}$$

$$\Lambda_2 = \left(1-\Gamma_p\Gamma_s T_p^2\right)(1-\Gamma_p\Gamma_s) + (\Gamma_s-\Gamma_p)\left(\Gamma_p T_p^2 - \Gamma_s\right) T_s^2. \tag{20}$$

2.4. Derivation of Constitutive Parameters

In the formulation, it is assumed that we know the electrical properties (ε_p and μ_p) and the length (L_p) of the movable plug and the length of the waveguide holder $L_g = L + L_p + L_0$. Because of the asymmetry of the measurement cell (sample, movable plug, and air) inside the calibration plane in Fig. 2, we could not directly apply the Nicolson-Ross-Weir (NRW) technique [9, 10]. Instead, we obtain a different formulation as follows.

We first express T_s^2 in terms of Γ_s using S_{11} in (12) as

$$T_s^2 = \frac{\left(1-\Gamma_p\Gamma_s T_p^2\right)\left[(\Gamma_s-\Gamma_p) - (1-\Gamma_p\Gamma_s)\, S_{11}\right]}{\left(\Gamma_p T_p^2 - \Gamma_s\right)\left[(\Gamma_s-\Gamma_p)\, S_{11} - (1-\Gamma_p\Gamma_s)\right]}. \tag{21}$$

Next, we substitute T_s in (21) into (18)–(20) and find a function depending on Γ_s, Γ_p, and T_p as

$$F(\Gamma_s, \Gamma_p, T_p) = \frac{\Lambda_3\left(1-\Gamma_s^2\right)^2\left(\Gamma_p\Gamma_s T_p^2 - 1\right)\Omega_1}{\Omega_2\left(\Gamma_p\Gamma_s - 1\right)^2} = 0, \tag{22}$$

where

$$\Lambda_3 = \left(\Gamma_p^2 - 1\right)^2, \quad U = S_{21}^2/S_{22}, \tag{23}$$

$$\Lambda_4 = \left[\left((U - S_{11} - \Gamma_p)\, S_{11} - 1\right)\Gamma_p - S_{11}\right] T_p^2, \tag{24}$$

$$\Lambda_5 = \left[\left((S_{11}-U)\, S_{11} + 1\right)\Gamma_p + \left(T_p^2 - 2\right) U + 4S_{11}\right] \Gamma_p T_p^2 + \left(1 + (S_{11}-U)\, S_{11}\right) T_p^2 + U\Gamma_p. \tag{25}$$

$$\Omega_1 = \Lambda_4\Gamma_s^2 + \Lambda_5\Gamma_s + \Lambda_4, \tag{26}$$

$$\Omega_2 = \left(\Gamma_s - \Gamma_p T_p^2\right)\left[(S_{11}+\Gamma_p)\,\Gamma_s - S_{11}\Gamma_p - 1\right]^2. \tag{27}$$

After some functional analysis, it is observed that among the numerator terms, only $\Omega_1 = 0$ satisfies the equation in (22). This is because a solution for Γ_s must change with different L. Therefore, the explicit expression for Γ_s will be

$$\Gamma_{s(1,2)} = \left(-\Omega_3 \mp \sqrt{\Omega_3^2 - 4}\right)/2, \quad \Omega_3 = \Lambda_5/\Lambda_4. \tag{28}$$

The correct root of Γ_s from (28) can be selected by imposing $|\Gamma_s| \leq 1$. After determining Γ_s, T_s can be calculated by substituting that Γ_s into (21). Then, we can determine L_0 using either (13) or (14). Finally, L, ε_r, and μ_r will be

$$L = L_g - L_p - L_0, \quad \frac{1}{\Lambda^2} = \left(\frac{j}{2\pi L}\ln(T_s)\right)^2, \tag{29}$$

$$\mu_r = \mu_p \frac{(1+\Gamma_s)}{(1-\Gamma_s)} \frac{\lambda_0}{\Lambda\sqrt{\varepsilon_p\mu_p - f_{c1}^2/f^2}}, \tag{30}$$

$$\varepsilon_r = \lambda_0^2\left(1/\Lambda^2 + f_{c1}^2/f^2\right)/\mu_r. \tag{31}$$

In addition to the advantage that the method explicitly measures the ε_r and μ_r when L and L_0 are unknown, it does not suffer from any unequal lengths of the plugs and un-identical plugs used for holding the liquid samples [14]. This is because it requires the knowledge on the length and constitutive parameters of only the movable plug.

In the derivation of ε_r and μ_r, we have used S-parameters presentation of the whole microwave network between the calibration plane in Fig. 1. Instead, we could have used transmission (ABCD) matrix or wave-cascading matrix (WCM) presentations [34–36] to derive the same expressions for ε_r and μ_r in (30) and (31).

3. RESULTS

A general purpose waveguide measurement set-up is used for validation of the proposed method [24–27]. A HP8720C VNA is connected as a source and measurement equipment. It has a 1 Hz frequency resolution (with option 001) and 8 ppm (parts per million) frequency accuracy. The waveguide used in measurements has a width of 22.86 mm ($f_c \cong$ 6.555 GHz).

The thru-reflect-line (TRL) calibration technique [37] is utilized before measurements. We used a waveguide short and the shortest waveguide spacer ($44.38 \mp 5\%$ mm) in our lab for reflect and line standards, respectively. The line has a $\pm 70^\circ$ maximum offset from 90°

between 9.7 GHz and 11.7 GHz. After calibration, we applied time-domain gating to decrease post reflections and to obtain smoother complex S-parameter measurements.

We utilized two 10 mm polytetrafluoro-ethylene (PTFE) samples as plugs for holding thin solid and liquid samples in place so that there will be no meniscus formation on surfaces of liquid samples and there will be no sagging of solid samples. We measured the ε_p of the PTFE samples by a broadband and stable transmission-reflection method [26] while only the PTFE sample is present inside the holder, and found $\varepsilon_p \cong 2.042 - j0.0014$ over 9.7–11.7 GHz. We used distilled water and a commercially available antifreeze solution as liquid test samples and 1 mm and 2 mm thin Plexiglas samples as solid test samples to validate the method. Figs. 3–5 demonstrate the measured ε_r of these samples over 9.7–11.7 GHz.

It is seen from Fig. 3 that both real and imaginary parts of the measured ε_r of distilled water are in good agreement with those computed from the Debye model [38]. For comparison of our proposed method with another waveguide method (plug-loaded two-port transmission line (PLTL) [14]), we also measured the ε_r of an antifreeze solution by this method. Fig. 4 illustrates the measured ε_r of an antifreeze solution over 9.7–11.7 GHz by our method and by the PLTL method. It is seen from Fig. 4 that real and imaginary parts of the measured ε_r of an antifreeze solution by both methods are in very good agreement with each other. We kept the distances between calibration plane and end surface of the movable plug minimum so that

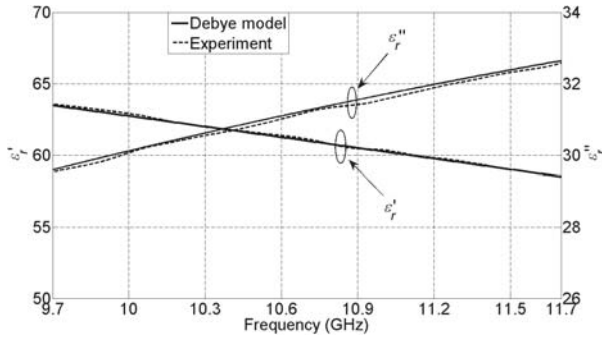

Figure 3. (a) Real part and (b) imaginary part of the measured (dashed line) and theoretical (solid line) ε_r of distilled water over 9.7–11.7 GHz. The parameters for the Debye model are $\varepsilon_\infty = 5.2$, $\varepsilon_s = 78.5$, and relaxation time, $\tau = 8.3$ ps at room temperature (20–25°C) [38].

we could easily measure them by the PLTL method. In our proposed method, we eliminate this necessity using (12) and (18).

In order to test our proposed method for measurements of thin solid materials, we measured the solid test samples over 9.7–11.7 GHz. The measurement result is shown in Fig. 5. It is seen from this figure that measured ε_r of both Plexiglas samples are in good agreement with the published reference data [39, 40]. At ordinary room temperature, the ε_r of the Plexiglas sample given by Von Hippel is approximately $2.59 - j0.0174$ at 10 GHz [40]. While ε_r' of both samples have a smooth dependency over the frequency band, ε_r'' of these samples have some oscillatory behaviour, especially for 1 mm Plexiglas sample. This is because longer samples are more homogenous than shorter ones. In addition, we observed that although the proposed method in [27]

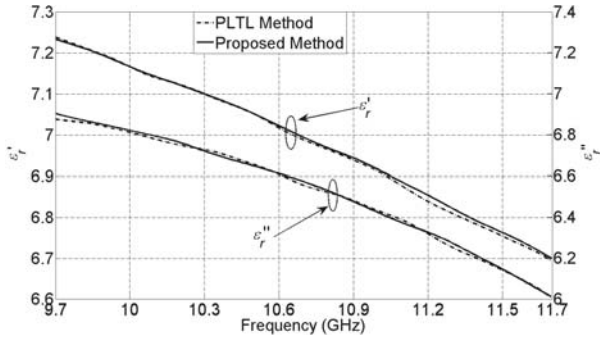

Figure 4. (a) Real part and (b) imaginary part of the measured ε_r of an antifreeze solution over 9.7–11.7 GHz by the plug-loaded two-port transmission line (PLTL) method [14] and by the proposed method.

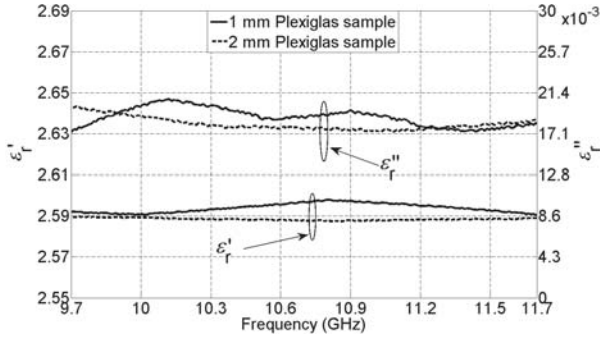

Figure 5. Measured ε_r of thin solid test samples (1 mm and 2 mm long Plexiglas samples) over 9.7–11.7 GHz by the proposed method.

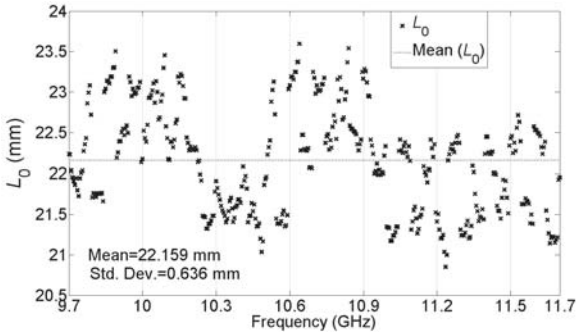

Figure 6. Dependency of the computed length of air–filled section, L_0, inside the proposed sample holder for a commercially available antifreeze solution over frequency.

results in accurate ε_r values of thin solid samples, it is not very feasible for very thin samples due to sample sagging. This problem is eliminated by the proposed method in this study.

As a self-checking feature of our method, the dependency of computed L_0 can be drawn over the frequency band to evaluate the correctness of extracted constitutive parameters of and/or the homogeneity of samples. For example, Fig. 6 shows this dependency for measurements of the commercially available antifreeze solution over 9.7–11.7 GHz. It is observed that the standard deviation (Std. Dev. = 0.636 mm) of the computed L_0 is little higher than that of the air section length of another sample holder operating at 3 GHz [22]. The reason for this can be the higher frequencies (approximately 10.7 GHz) used for testing our proposed holder.

4. CONCLUSION

An accurate and very promising microwave method is proposed for explicit constitutive parameters determination of thin solid and liquid materials. The method eliminates the dependency of calibration plane and the need for precise information on the length of the sample by using full scattering parameter measurements while explicitly measuring the constitutive parameters. It readily lends itself for automated measurements using a vector network analyzer. In addition, it also proposes a self-checking feature to monitor the accuracy and performance of measurements regardless of the electrical properties of samples. For validation of the method, we measured the complex permittivity of some thin solid and liquid test samples.

ACKNOWLEDGMENT

U. C. Hasar (Mehmetcik) would like to thank TUBITAK (The Scientific and Technological Research Council of Turkey) Münir Birsel National Doctorate Scholarship and YOK (The Higher Education Council of Turkey) Doctorate Scholarship for supporting his studies.

REFERENCES

1. Nyfors, E. G. and P. Vainikainen, *Industrial Microwave Sensors*, Artech House, Inc., Norwood, MA, 1989.
2. Chen, L. F., C. K. Ong, C. P. Neo, et al., *Microwave Electronics: Measurement and Materials Characterization*, John Wiley & Sons, West Sussex, England, 2004.
3. Hebeish, A. A., M. A. Elgamel, R. A. Abdelhady, et al., "Factors affecting the performance of the radar absorbant textile materials of different types and structures," *Progress In Electromagnetics Research B*, Vol. 3, 219–226, 2008.
4. Zhang, H., S. Y. Tan, and H. S. Tan, "An improved method for microwave nondestructive dielectric measurement of layered media," *Progress In Electromagnetics Research B*, Vol. 10, 145–161, 2008.
5. Pozar, D. M., *Microwave Engineering*, John Wiley & Sons, Inc., New York, NY, 2005.
6. Rubinger, C. P. L. and L. C. Costa, "Building a resonant cavity for the measurement of microwave dielectric permittivity of high loss materials," *Microwave Opt. Tech. Lett.*, Vol. 49, 1687–1690, 2007.
7. Williams, T. C., M. A. Stuchly, and P. Saville, "Modified transmission-reflection method for measuring constitutive parameters of thin flexible high-loss materials," *IEEE Trans. Microw. Theory Tech.*, Vol. 51, 1560–1566, 2003.
8. Courtney, C. C. and W. Motil, "One-port time-domain measurement of the approximate permittivity and permeability of materials," *IEEE Trans. Microw. Theory Tech.*, Vol. 47, 551–555, 1999.
9. Weir, W. B., "Automatic measurement of complex dielectric constant and permeability at microwave frequencies," *Proc. IEEE*, Vol. 62, 33–36, 1974.
10. Nicolson, A. M. and G. Ross, "Measurement of the intrinsic properties of materials by time-domain techniques," *IEEE Trans. Instrum. Meas.*, Vol. 19, 377–382, 1970.

11. Packard, H., "Measuring dielectric constant of solids with the HP 8510 network analyzer," Product Note 8510-3, 1985.
12. Baker-Jarvis, J., E. J. Vanzura, and W. A. Kissick, "Improved technique for determining complex permittivity with the transmission/reflection method," *IEEE Trans. Microw. Theory Tech.*, Vol. 38, 1096–1103, 1990.
13. Baker-Jarvis, J., M. D. Janezic, J. H. Grosvenor, Jr., and R. G. Geyer, "Transmission/reflection and short–circuit line methods for measuring permittivity and permeability," NIST, Boulder, CO, Tech. Note 1355, 1992.
14. Bois, K. J., L. F. Handjojo, A. D. Benally, K. Mubarak, and R. Zoughi, "Dielectric plug-loaded two-port transmission line measurement technique for dielectric property characterization of granular and liquid materials," *IEEE Trans. Instrum. Meas.*, Vol. 48, 1141–1148, 1999.
15. Wang, Y. and M. N. Afsar, "Measurement of complex permittivity of liquids using waveguide techniques," *Progress In Electromagnetics Research*, PIER 42, 131–142, 2003.
16. Folgero, K., "Broad-band dielectric spectroscopy of low-permittivity fluids using one measurement cell," *IEEE Trans. Instrum. Meas.*, Vol. 47, 881–885, 1998.
17. Qaddoumi, N., S. Ganchev, and R. Zoughi, "Microwave diagnosis of low density glass fibers with resin binder," *Res. Nondestruc. Eval.*, Vol. 8, 177–188, 1996.
18. Hasar, U. C., "Calibration-independent method for complex permittivity determination of liquid and granular materials," *Electron. Lett.*, Vol. 44, 585–587, 2008.
19. Baker-Jarvis, J., M. D. Janezic, and C. A. Jones, "Shielded open-circuited sample holder for dielectric measurements of solids and liquids," *IEEE Trans. Instrum. Meas.*, Vol. 47, 338–344, 1998.
20. Vanzura, E. J., J. Baker-Jarvis, J. H. Grosvenor, and M. Janezic, "Intercomparison of permittivity measurements using the transmission/reflection method in 7-mm coaxial transmission lines," *IEEE Trans. Microw. Theory Tech.*, Vol. 42, 2063–2070, 1994.
21. Mattar, K. E., D. G. Watters, and M. E. Brodwin, "Influence of wall contacts on measured complex permittivity spectra at coaxial line frequencies," *IEEE Trans. Microw. Theory Tech.*, Vol. 39, 532–537, 1991.
22. Somlo, P. I., "A convenient self-checking method for the automated microwave measurement of μ and ε," *IEEE Trans.*

Instrum. Meas., Vol. 42, 213–216, 1993.

23. Sjöberg, D., "Determination of propagation constants and material data from waveguide measurements," *Progress In Electromagnetics Research B*, Vol. 12, 163–182, 2009.
24. Hasar, U. C., "Two novel amplitude-only methods for complex permittivity determination of medium- and low-loss materials," *Meas. Sci. Techol.*, Vol. 19, 055706–055715, 2008.
25. Hasar, U. C., "A fast and accurate amplitude-only transmission-reflection method for complex permittivity determination of lossy materials," *IEEE Trans. Microw. Theory Tech.*, Vol. 56, 2129–2135, 2008.
26. Hasar, U. C. and C. R. Westgate, "A broadband and stable method for unique complex permittivity determination of low-loss materials," *IEEE Trans. Microw. Theory Tech.*, Vol. 57, 471–477, 2009.
27. Hasar, U. C. and O. Simsek, "An accurate complex permittivity method for thin dielectric materials," *Progress In Electromagnetics Research*, PIER 91, 123–183, 2009.
28. Buyukozturk, O., T.-Y. Yu, and J. A. Ortega, "A methodology for determining complex permittivity of construction materials based on transmission-only coherent, wide-bandwidth free-space measurements," *Cem. Concr. Compos.*, Vol. 28, 349–359, 2006.
29. Ebara, H., T. Inoue, and O. Hashimoto, "Measurement method of complex permittivity and permeability for a powdered material using a waveguide in microwave band," *Sci. Technol. Adv. Mat.*, Vol. 7, 77–83, 2006.
30. Press, W. H., S. A. Teukolsky, W. T. Vetterling, and B. P. Flannery, *Numerical Recipes in C: The Art of Scientific Computing*, Cambridge University Press, New York, 1992.
31. Balanis, C. A., *Advanced Engineering Electromagnetics*, John Wiley & Sons, New Jersey, NJ, 1989.
32. Deshpande, M. D., C. J. Reddy, P. I. Tiemsin, and R. Cravey, "A new approach to estimate complex permittivity of dielectric materials at microwave frequencies using waveguide measurements," *IEEE Trans. Microw. Theory Tech.*, Vol. 45, 359–365, 1997.
33. Nishikata, A., "A swept-frequency measurement of complex permittivity and complex permeability of a columnar specimen inserted in a rectangular waveguide," *IEEE Trans. Microw. Theory Tech.*, Vol. 55, 1554–1567, 2007.
34. He, X., Z. Tang, B. Zhang, and Y. Wu, "A new deembedding method in permittivity measurement of ferroelectric thin film

material," *Progress In Electromagnetics Research Letters*, Vol. 3, 1–8, 2008.

35. Wu, Y., Z. Tang, Y. Yu, and X. He, "A new method to avoid acrowding phenomenon in extracting the permittivity of ferroelectric thin films," *Progress In Electromagnetics Research Letters*, Vol. 4, 159–166, 2008.
36. Hasar, U. C. and O. Simsek, "A simple approach for evaluating the reciprocity of materials without using any calibration standard," *Progress In Electromagnetics Research*, PIER 91, 139–152, 2009.
37. Engen, G. F. and C. A. Hoer, "'Thru-reflect-line': An improved technique for calibrating the dual six-port automatic network analyzer," *IEEE Microw. Theory and Tech.*, Vol. 27, 987–993, 1979.
38. Hasted, J. B., *Aqueous Dielectrics*, Chapman and Hall, London, UK, 1973.
39. Chin, G. Y. and E. A. Mechtly, "Properties of materials," *Reference Data for Engineering: Radio, Electronics, Computer, and Communications*, E. C. Jordan (ed.), 4-20–4-23, Howard W. Sams & Co., Indianapolis, IN, 1986.
40. Von Hippel, A. R., *Dielectric Materials and Applications*, 134–135, 310–332, John Wiley & Sons, New York, NY, 1954.